

## Optimization of $C^{5+}$ Balmer- $\alpha$ line intensity at 182 Å from laser-produced carbon plasma

A CHOWDHURY, R A JOSHI, P A NAIK and P D GUPTA

Laser Plasma Division, Raja Ramanna Centre for Advanced Technology, Indore 452 013, India

E-mail: avijit@cat.ernet.in

MS received 6 February 2006; revised 29 June 2006; accepted 22 August 2006

**Abstract.** Parametric dependence of the intensity of 182 Å Balmer- $\alpha$  line ( $C^{5+}; n = 3 \rightarrow 2$ ), relevant to xuv soft X-ray lasing schemes, from laser-produced carbon plasma is studied in circular spot focusing geometry using a flat field grating spectrograph. The maximum spectral intensity for this line in space integrated mode occurred at a laser intensity of  $1.2 \times 10^{13} \text{ W cm}^{-2}$ . At this laser intensity, the space resolved measurements show that the spectral intensity of this line peaks at  $\sim 1.5 \text{ mm}$  from the target surface indicating the maximum population of  $C^{5+}$  ions ( $n = 3$ ), at this distance. From a comparison of spatial intensity variation of this line with that of  $C^{5+}$  Ly- $\alpha$  ( $n = 2 \rightarrow 1$ ) line, it is inferred that  $n = 3$  state of  $C^{5+}$  ions is predominantly populated through three-body recombination pumping of  $C^{6+}$  ions of the expanding plasma consistent with quantitative estimates on recombination rates of different processes.

**Keywords.** xuv-spectroscopy; laser-produced plasma; flat-field grating spectrograph; Nd:phosphate glass laser.

**PACS Nos** 52.25.Jm; 52.50.Jm; 52.70.La

Intense xuv soft X-ray radiation from pulsed laser plasma sources is of current interest for a variety of research investigations and technological applications [1–5]. Measurements of xuv radiation spectrum of laser-produced plasmas with high spectral, temporal and spatial resolutions is an essential part of many studies of laser plasma interaction, particularly for investigations of xuv soft X-ray lasing schemes [6]. The first recombinational X-ray laser was demonstrated in laser-produced carbon plasma at 182 Å Balmer- $\alpha$  transition ( $C^{5+}; n = 3 \rightarrow 2$ ) with line focusing geometry [7]. Study of population of  $C^{5+}$  ions in the upper state of this transition (i.e.  $n = 3$  state) is a prerequisite to determine appropriate laser irradiation and target parameters for optimizing recombinational carbon X-ray laser [6]. A knowledge of the spatial location of the plasma region of maximum  $C^{5+}$  ion density is an important aspect in this regard. The study can be carried out in circular focal spot geometry and the results can be used later for cylindrical focusing geometry required for X-ray lasing experiments.

Here we report an experimental study on space integrated and space resolved spectral line intensity measurement of Balmer- $\alpha$  line from a laser-produced carbon plasma using a flat-field grating spectrograph. In space integrated mode we present the results on the variation of spectral line intensity with laser intensity to find the optimum laser intensity. At this optimum intensity, we have studied the spatial variation of spectral intensity away from the target surface to determine the location of maximum line intensity. Results of both these studies can be used for line focusing geometry.

Experiments were performed using a 2.5 GW, 4 ns Nd:phosphate glass laser system. The laser beam ( $\lambda = 1.054 \mu\text{m}$ ) was focused normally on a planar polyethylene target using a 400 mm plano-convex lens in a plasma chamber evacuated to  $10^{-4}$  Torr. The focal spot diameter was  $\sim 100 \mu\text{m}$ . Space integrated as well as space resolved xuv emission spectra from the plasma were recorded using a flat field grating spectrograph [8]. The spectrograph is based on a variable groove-spacing grating with nominal groove number of 1200 1/mm for achieving flat field focusing. The distance between source and entrance slit was 60 mm whereas slit to grating and grating to film distance were 237 mm and 235 mm respectively. The width and height of the entrance slit were  $50 \mu\text{m}$  and 3 mm respectively. The spectrograph was mounted at right angles to the direction of the laser beam. The spectra were recorded on UFSH-4 Russian X-ray films and were developed in a D-19 developer and fixed with standard acid fixer.

In the space integrated mode of our spectrograph [8], the entrance slit was kept perpendicular to the plasma expansion direction. We have used this mode to study the variation of  $\text{C}^{5+}$  Balmer- $\alpha$  line intensity with laser intensity to determine the optimum laser intensity for maximum population of  $\text{C}^{5+}$  ions in the upper state of this transition (i.e.  $n = 3$  state). The space integrated spectrum of carbon plasma at a laser intensity of  $7 \times 10^{12} \text{ W cm}^{-2}$  is shown in figure 1a. Some prominent lines in the spectral region of our interest are identified [9] to be fourth and fifth order of He- $\alpha$  line ( $40.3 \text{ \AA}$ ) of  $\text{C}^{4+}$  ions respectively at  $161.2 \text{ \AA}$  and  $201.5 \text{ \AA}$ . The intense line between these two lines is the  $182 \text{ \AA}$  line whereas the faint line next to it is the  $186 \text{ \AA}$  line ( $\text{C}^{4+} 1s4d \rightarrow 1s2p$ ).

For space resolved mode of operation, firstly the spectrograph was rotated  $90^\circ$  about its axis in such a way that the grating surface faced upwards. In this configuration the entrance slit is kept parallel to the plasma expansion direction. Necessary changes were made in the octagonal plasma chamber flange in which spectrograph was mounted. Next, an additional slit (for spatial resolution), was placed perpendicular to the direction of the entrance slit (between the grating and the plasma chamber flange) inside the grating chamber. This space resolving slit of  $150 \mu\text{m}$  width was located at a distance of 40 mm from the grating center and towards the detector side. The height of this slit was kept long  $\sim 20 \text{ mm}$ , so that it allows all the diffracted rays to pass through it. A spatial resolution of  $\sim 250 \mu\text{m}$  was available with this configuration. We have used this mode to study the axial variation of Balmer- $\alpha$   $182 \text{ \AA}$   $\text{C}^{5+}$  line intensity in the direction of the target normal (which is also the plasma expansion direction). The space resolved spectrum recorded at a laser intensity of  $7 \times 10^{12} \text{ W cm}^{-2}$  is shown in figure 1b. It may be noted that whereas in space integrated mode (figure 1a) one gets spectral lines, the space resolved spectrum depicts the shape of the emission region of various lines.

Optimization of  $C^{5+}$  Balmer- $\alpha$  line intensity

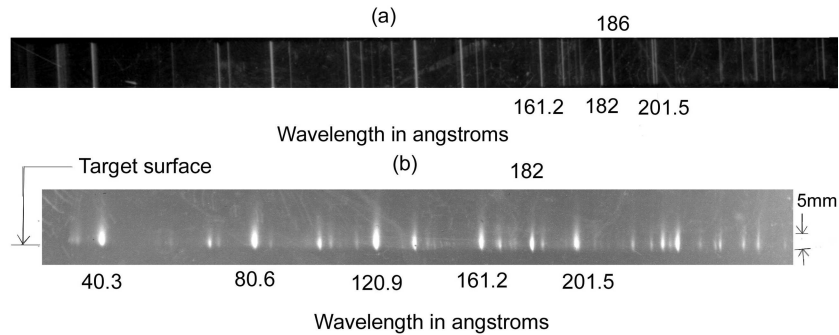


**Figure 1.** (a) Space integrated emission spectrum of carbon plasma. Fourth and fifth order of He- $\alpha$  (40.3 Å) line of  $C^{4+}$  ion along with 182 Å and 186 Å lines are indicated. (b) Space resolved emission spectrum of carbon plasma. First to fifth order of He- $\alpha$  (40.3 Å) lines are marked along with 182 Å line.

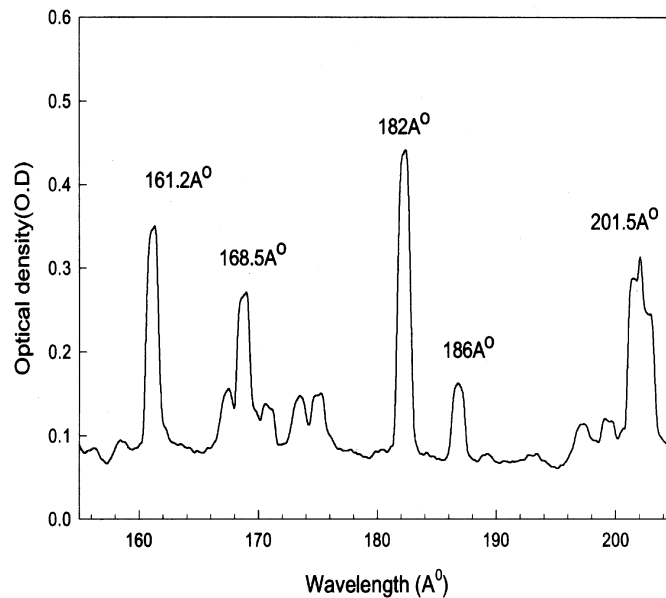


**Figure 2.** Densitometer scan of the spectrum in figure 1a between 155 Å and 205 Å.

A densitometric trace between 155 Å and 205 Å of figure 1a is shown in figure 2. Fourth (161.2 Å) and fifth (201.5 Å) order of He- $\alpha$  line (40.3 Å) of  $C^{4+}$  ion along with the 182 Å and 186 Å lines are identified in this figure. The optical density (OD) of the spectral lines was read by a microdensitometer and converted to intensity ( $I_\lambda$ ) using the relation,  $I_\lambda = 10^{OD/\gamma}$ , where  $\gamma$  is the contrast ratio of the film. Since the contrast ratio of the UFSH-4 film for 182 Å was not available in the literature, it was determined experimentally. This was done from measurements of optical density vs. exposure for the neighboring line at  $\lambda = 186$  Å. This line was

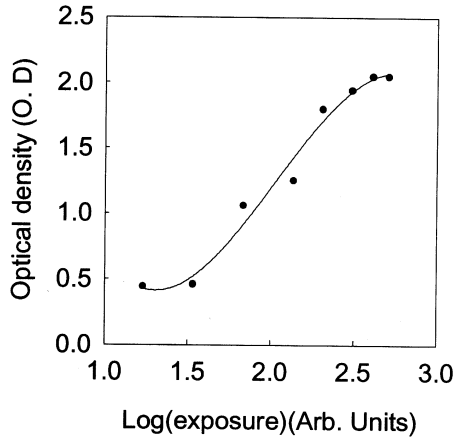


**Figure 3.** Variation of optical density with log (exposure) of UFSH-4 xuv film.

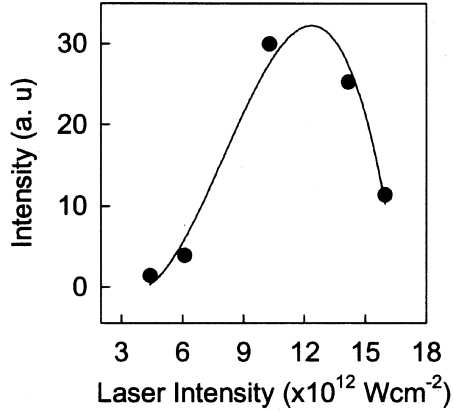


**Figure 4.** Space integrated intensity variation of the 182 Å line with laser intensity.

chosen as it is a clearly identifiable line close to 182 Å line and it has a much lower intensity compared to the 182 Å line. Thus a large range of optical density can be covered by exposing the film with different number of laser shots.

The measurement was carried out by multiple shot exposure technique, where laser-produced plasma acted as a source of 186 Å line for exposing the film. Different areas of the film were exposed to different number of shots, thereby producing different optical densities (OD) leading to the Hurter and Driffield (H-D) curve for the film. OD values of 0.44, 0.46, 1.06, 1.25, 1.8, 1.94, 2.05 and 2.05 were obtained with 2, 4, 8, 16, 24, 36, 48 and 60 number of shots respectively with each shot of energy approximating to 8.5 J. From this data H-D curve (OD vs. log(exposure)) for the film is plotted in figure 3. From this figure, the value of contrast ratio  $\gamma$  is determined to be 1.5 which is the slope of the straight line portion. Using this value of  $\gamma$  we have calculated the intensity of 182 Å line from the measured OD values.

The variation of the space integrated intensity of 182 Å line with laser intensity is shown in figure 4. It is seen from this figure that the intensity of this line initially increases and reaches a peak at a certain laser intensity and then decreases with further increase in laser intensity. The optimum laser intensity for the maximum spectral intensity of this line is  $1.2 \times 10^{13} \text{ W cm}^{-2}$  (corresponding to  $\sim 6.5 \text{ J}$  laser energy). This implies that the maximum population of  $\text{C}^{5+}$  ions in  $n = 3$  state is produced at this laser intensity. This behavior can be physically explained by noting that as the temperature of the plasma increases with the increase of laser intensity, the population density of these ions increases but further increase in temperature beyond a certain value will lead to further ionization [10,11] to  $\text{C}^{6+}$  thereby reducing the population density of  $\text{C}^{5+}$  ions. The laser energy corresponding to the optimum laser intensity for cylindrically-shaped plasma required for X-ray lasing experiment will increase proportionally with the increase in the area of the focal region.

Next, the spectrograph was set for space resolved operation and space resolved spectrum was recorded for the above determined optimum laser intensity of  $1.2 \times$

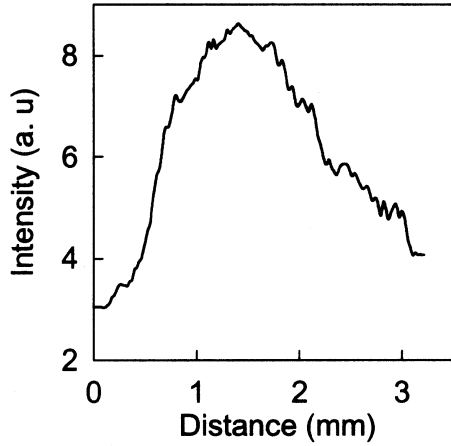


**Figure 5.** Spatial intensity variation of the  $C^{5+}$   $n = 3 \rightarrow 2$  182 Å line in the direction of target normal.

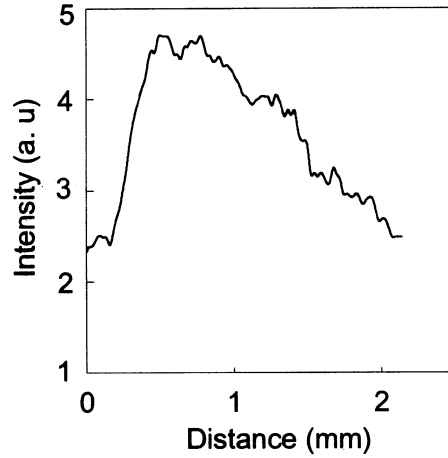


**Figure 6.** Spatial intensity variation of the  $C^{4+}$ :  $1s2p \rightarrow 1s^2$  33.7 Å line.

$10^{13} \text{ W cm}^{-2}$ . The variation of the spectral intensity of this 182 Å line with distance from the target surface is shown in figure 5. It is seen from this figure that the emission of this line extends up to  $\sim 2.8$  mm from the target surface. It first increases up to  $\sim 1.5$  mm and then monotonically decreases to the background level. In order to get a better insight into the processes resulting in pumping of the upper state of the 182 Å line transition ( $C^{5+}:n = 3$ ), it may be useful to examine the space resolved intensity of one more line, viz.  $C^{5+}$  Ly- $\alpha$  ( $n = 2 \rightarrow 1$ ) at  $\lambda = 33.7$  Å. Spatial variation of intensity of this line along the target normal is shown in figure 6. The  $\gamma$  value for this line is taken from [12]. It is seen from figure 6 that the line intensity first increases, reaches a maximum at  $\sim 0.5$  mm, and then decreases reaching the background level at  $\sim 2$  mm. This indicates that the density and temperature condition of the plasma ceases to support sufficient electron collisional excitation to  $n = 2$  level of  $C^{5+}$  ions beyond 0.7 mm since the Ly- $\alpha$  intensity decreases beyond this distance. Hence the collisional excitation to  $n = 3$  level will be even smaller beyond 0.7 mm. This can be easily seen by taking the temperature scaling with distance from the target surface. In plasma produced from solid targets by multಿನanosecond laser pulses, the peak temperature region is located at a certain distance from the target surface where the plasma expansion departs from one-dimensional expansion [13]. The latter becomes significant at a distance equal to the focal spot radius. Estimates based on steady state plasma production model applicable to long pulse irradiation provides a maximum temperature of  $\sim 450$  eV [13] near the critical density ( $\sim 1.1 \times 10^{27} \text{ m}^{-3}$ ) at the laser intensity of  $1.2 \times 10^{13} \text{ W cm}^{-2}$ . Thus to get approximate estimates, one may take the location of the region of peak temperature and critical density of plasma at a distance of  $\sim 50 \mu\text{m}$  from the target. Using temperature scaling with distance ( $r$ ) from the target surface in the expansion zone as  $r^{-2}$  [14], one gets a temperature of  $\sim 2.3$  eV at 0.7 mm from the target surface. At this temperature, the collisional excitation to  $n = 3$  (energy

430.5 eV) and  $n = 2$  (energy 367.9 eV) from the ground state, that is  $n = 1$  will be  $\sim e^{-27}$  for 2.3 eV. Thus, the increase in spatial intensity of 182 Å line occurring at a distance of 0.7 mm may be attributed to plasma recombination processes [15–18].

In general, processes of recombination in a plasma include radiative recombination, three-body recombination and dielectronic recombination. The latter for a fully ionized  $C^{6+}$  ion is absent. The relative contribution of the other two processes can be estimated by calculating their rates. The rates of radiative ( $R_r$ ) and three-body recombination ( $R_{3b}$ ) processes are respectively given by [19]

$$R_r = 2.7 \times 10^{-19} n_e n_i Z^2 T_{eV}^{-3/4} \quad (1)$$

and

$$R_{3b} = 9.2 \times 10^{-39} n_e^2 n_i Z^3 T_{eV}^{-9/2} \ln \sqrt{Z^2 + 1}, \quad (2)$$

where  $n_e$  and  $n_i$  are the electron and ion density in cubic meter and  $T_{eV}$  is the electron temperature in electron Volts and  $Z$  is the ionic charge. Taking the variation of electron density with distance from the target surface  $r$  as  $n_e \sim r^{-3}$  [14], gives an electron density of  $\sim 4 \times 10^{23} \text{ m}^{-3}$  at a distance of 0.7 mm from the target surface. Hence the relative contribution of radiative recombination to three-body recombination at 0.7 mm using eqs (1) and (2) is found to be  $\sim 1.5 \times 10^{-4}$ . Thus in the expansion zone of the plasma that we are dealing with, the three-body recombination is dominant over the radiative recombination. Further, this recombination takes place preferably at higher quantum levels  $n$  where the energy of that level  $E_n \sim T_{eV}$  [15]. Considering  $E_n \sim \frac{13.6Z^2}{n^2}$  eV (where  $Z$  is the atomic number) and using  $T_{eV} \sim 2.3$  eV, the value of  $n$  is  $\sim 14$ . Thus the electrons preferably recombine at higher quantum levels by three-body recombination and percolates down to the lower quantum levels. It may therefore be inferred that the  $n = 3$  state of  $C^{5+}$  ions is predominantly populated through three-body recombination pumping of  $C^{6+}$  ions in the expansion zone.

In conclusion, we have studied the spatial intensity variation of  $C^{5+}$   $n = 3 \rightarrow 2$ , 182 Å line in circular spot focus geometry by setting up a flat field grating spectrograph. Optimum laser intensity for maximum population of  $C^{5+}$  ions in  $n = 3$  state was found to be  $1.2 \times 10^{13} \text{ W cm}^{-2}$  from space integrated measurement. The space resolved intensity of the 182 Å line recorded for this laser intensity showed that the peak population occurs at  $\sim 1.5$  mm from the target surface. From a comparison of spatial variation of this line with that of  $C^{5+}$  Ly- $\alpha$  ( $n = 2 \rightarrow 1$ ) line, it may be inferred that  $n = 3$  state of  $C^{5+}$  ions is predominantly populated through three-body recombination pumping of  $C^{6+}$  ions of the expanding plasma consistent with quantitative estimation of recombination rates. Necessary calibration of the the film used was also done.

## References

- [1] I C E Turcu and J B Dance, in *X-rays from laser plasmas: Generation and applications* (Wiley, New York, 1999)
- [2] J Lindl, *Phys. Plasmas* **2**, 3933 (1995)

*Optimization of  $C^{5+}$  Balmer- $\alpha$  line intensity*

- [3] M Chaker *et al*, *J. Vac. Sci. Technol.* **B10**, 3293 (1992)
- [4] J Chakera, S R Kumbhare and P D Gupta, *J. X-ray Sci. Technol.* **8**, 1 (1998)
- [5] R A Ganeev, J A Chakera, M Raghuramaiah, A K Sharma, P A Naik and P D Gupta, *Phys. Rev.* **A63**, 026402 (1-6) (2001)
- [6] H Diado, *Rep. Prog. Phys.* **65**, 1513 (2002)
- [7] S Suckewer *et al*, *Phys. Rev. Lett.* **55**, 1753 (1985)
- [8] A Chowdhury, R A Joshi, S R Kumbhare, P A Naik and P D Gupta, *Sadhana* **24**, 557 (1999)
- [9] R L Kelly and L J Palumbo, *Atomic and ionic emission lines below 2000 Å*, Naval Research Laboratory Report No. 7599 (Naval Research Laboratory, Washington, D.C., 1973)
- [10] A Chowdhury, R A Joshi, G P Gupta, P A Naik and P D Gupta, *Pramana – J. Phys.* **61**, 1121 (2003)
- [11] A Chowdhury, G P Gupta, P A Naik and P D Gupta, *Pramana – J. Phys.* **64**, 141 (2005)
- [12] Y M Alexandrov *et al*, *Nucl. Instrum. Methods Phys. Res.* **A308**, 343 (1991)
- [13] P Mora, *Phys. Fluids* **25**, 1051 (1983)
- [14] P T Rumsby and J W M Paul, *Plasma Phys.* **16**, 247 (1974)
- [15] B Yu Zeldovich and P Yu Raizer, in *Physics of shock waves and high temperature hydrodynamic phenomena* (Academic Press, New York, 1966) vol. 1, p. 94
- [16] P A Naik, P D Gupta and S R Kumbhare, *Phys. Rev.* **A43**, 4540 (1991)
- [17] A Neogi and R K Thareja, *Phys. Plasmas* **6**, 365 (1999)
- [18] A Chowdhury, V Arora, P A Naik and P D Gupta, *J. Appl. Phys.* **93**, 3218 (2003)
- [19] R K Thareja, Abhilasha and R K Dwivedi, *Laser and Part. Beams* **13**, 481 (1995)